

Caspase-9 inhibition triggers Hsp90-based chemotherapy-mediated tumor intrinsic innate sensing and enhances antitumor immunity

Jingyang Li, Xiaoyu Han, Mayu Sun, Weida Li, Guanghuan Yang, Huiyi Chen, Bao Guo, Jingquan Li, Xiaoguang Li , Hui Wang 

To cite: Li J, Han X, Sun M, *et al.* Caspase-9 inhibition triggers Hsp90-based chemotherapy-mediated tumor intrinsic innate sensing and enhances antitumor immunity. *Journal for ImmunoTherapy of Cancer* 2023;11:e007625. doi:10.1136/jitc-2023-007625

► Additional supplemental material is published online only. To view, please visit the journal online (<http://dx.doi.org/10.1136/jitc-2023-007625>).

Jingyang Li, XH and MS contributed equally.

Accepted 09 November 2023



© Author(s) (or their employer(s)) 2023. Re-use permitted under CC BY-NC. No commercial re-use. See rights and permissions. Published by BMJ.

State Key Laboratory of Systems Medicine for Cancer, Center for Single-Cell Omics, School of Public Health, Shanghai Jiao Tong University School of Medicine, Shanghai, China

Correspondence to

Dr Xiaoguang Li;
lixg@shsmu.edu.cn

Dr Hui Wang;
huiwang@shsmu.edu.cn

ABSTRACT

Background Antineoplastic chemotherapies are dramatically efficient when they provoke immunogenic cell death (ICD), thus inducing an antitumor immune response and even tumor elimination. However, activated caspases, the hallmark of most cancer chemotherapeutic agents, render apoptosis immunologically silent. Whether they are dispensable for chemotherapy-induced cell death and the apoptotic clearance of cells *in vivo* is still elusive.

Methods A rational cell-based anticancer drug library screening was performed to explore the immunogenic apoptosis pathway and therapeutic targets under apoptotic caspase inhibition. Based on this screening, the potential of caspase inhibition in enhancing chemotherapy-induced antitumor immunity and the mechanism of actions was investigated by various cells and mouse models.

Results Heat shock protein 90 (Hsp90) inhibition activates caspases in tumor cells to produce abundant genomic and mitochondrial DNA fragments and results in cell apoptosis. Meanwhile, it hijacks Caspase-9 signaling to suppress intrinsic DNA sensing. Pharmacological blockade or genetic deletion of Caspase-9 causes tumor cells to secrete interferon (IFN)- β via tumor intrinsic mitochondrial DNA/the second messenger cyclic GMP-AMP (cGAS) /stimulator of interferon genes (STING) pathway without impairing Hsp90 inhibition-induced cell death. Importantly, both Caspase-9 and Hsp90 inhibition triggers an ICD, leading to the release of numerous damage-associated molecular patterns such as high-mobility group box protein 1, ATP and type I IFNs *in vitro* and remarkable antitumor effects *in vivo*. Moreover, the combination treatment also induces adaptive resistance by upregulating programmed death-ligand 1 (PD-L1). Additional PD-L1 blockade can further overcome this acquired immune resistance and achieve complete tumor regression.

Conclusions Blockade of Caspase-9 signaling selectively provokes Hsp90-based chemotherapy-mediated tumor innate sensing, leading to CD8⁺ T cell-dependent tumor control. Our findings implicate that pharmacological modulation of caspase pathway increases the tumor-intrinsic innate sensing and immunogenicity of chemotherapy-induced apoptosis,

and synergizes with immunotherapy to overcome adaptive resistance.

BACKGROUND

Although immunotherapy, especially immune checkpoint inhibitors, has shown clinical success, its efficacy is often limited.¹ Failure to effectively activate the immune system to generate durable antitumor activity often leads to incomplete tumor elimination and tumor recurrence.² A major factor in initial resistance to immunotherapy is the so-called “immunological cold” tumors, characterized by the absence of tumor-infiltrating lymphocytes.³ To overcome this challenge, immune-based combination therapies have emerged to establish a T cell-inflamed tumor microenvironment (TME) and enhance antitumor immune responses.⁴

A key functional feature of T cell-inflamed TME is the type I interferon (IFN) signature,⁵ which represents a key part of the initial phase of innate immunity. Type I IFNs play a crucial role in activating both innate and adaptive immunity, including dendritic cell maturation, antigen processing and presentation, and cross-priming of T cells.^{6,7} Studies have shown that type I IFN signature positively correlates with T-cell infiltration and clinical outcomes in various types of cancers,⁸ suggesting that activation of type I IFN signaling may represent a crucial mechanistic event in response to immunotherapy. Additionally, type I IFNs are potent inducers of immune checkpoint proteins,^{9–11} which are commonly used as predictive biomarkers of immunotherapeutic response. However, the expression of type I IFNs is often silenced or restricted within the TME.⁷ The stimulator of interferon genes (STING) is a well-characterized mediator in type I IFN production, which is activated by cytosolic DNA. Corresponding with type I IFN

silencing, STING signaling is also frequently functionally suppressed in a wide variety of cancers.¹² Deficiency in STING signaling limits innate sensing and is associated with poor prognosis and worse response to immunotherapy.^{13–15} Moreover, many conventional chemotherapeutics, targeted anticancer agents and immunological adjuvants are only fully efficient in the presence of intact type I IFN signaling.⁷ Therefore, enhancing STING and type I IFN signaling could be a promising strategy to improve the efficacy of immunotherapy.

Immunostimulatory chemotherapeutics are promising partners for combination regimens involving immune checkpoint inhibitors.¹⁶ One dogma might involve the induction of immunogenic cell death (ICD) that triggers type I IFN signaling and T-cell infiltration to enhance antitumor immunity.¹⁷ ICD is considered one of the most promising approaches to achieving total tumor cell elimination and long-term immunological memory.¹⁸ Although previous studies have proposed several immunogenic drugs (eg, oxaliplatin, cyclophosphamide) to trigger ICD and type I IFN production in tumor cells and improve the therapeutic efficacy of immunotherapy, most chemotherapeutic agents render cell apoptosis via immunological silencing that results in less inflammation.^{18–2018 to 20} Intrinsic apoptosis, initiated by mitochondrial outer membrane permeabilization (MOMP), is considered as one of the major mechanisms underlying the antitumor activities attributed to chemotherapeutic agents.^{21 22} Following MOMP, mitochondrial DNA (mtDNA) is released into the cytosol and sensed by the second messenger cyclic GMP-AMP (cGAS)/STING /interferon regulatory factor 3 (IRF3) pathway, producing type I IFNs. However, MOMP also causes cytochrome c release, which subsequently triggers caspase activation and facilitates the cleavage of cGAS and IRF3.²³ The apoptotic caspase-mediated cleavages rapidly impede innate sensing and suppress mtDNA-induced STING-mediated type I IFN production, thereby preserving the immunologically quiescent state of apoptosis.^{24 25} Although mtDNA release appears to be a routine event during intrinsic apoptosis, the mtDNA-induced type I IFN secretion is only apparent in the absence of caspases.^{26 27} Interestingly, accumulating studies indicate that activated caspases are dispensable for cell death and the apoptotic clearance of cells in vivo.²⁸ For example, Caspase-9-deficient cells exhibit only short-term resistance to apoptotic stimuli and do not determine drugs-treated cell death.²⁷ This raises an important question of whether blocking chemotherapy-induced caspase activation could switch the intrinsic apoptosis from the “immunosuppressive” to “immunogenic” state to facilitate better tumor control.

In this study, we proposed a cell-based anticancer drug library screening approach for exploring the immunogenic apoptosis pathway and therapeutic targets under apoptotic caspase inhibition. We identified heat shock protein 90 (Hsp90) as a novel and potent target for activating immunogenic apoptosis and antitumor immunity.

Blocking Hsp90-based chemotherapy-induced Caspase-9 activation provoked tumor intrinsic mtDNA sensing and T cell-inflamed TME for better tumor control. Notably, the combination treatment exhibited potent synergistic effects with programmed death-ligand 1 (PD-L1) blockade, even leading to complete tumor regression. Our findings highlight the potential of caspase inhibition in enhancing Hsp90-based chemotherapy-induced anti-tumor immunity and provide a novel therapeutic strategy to improve innate sensing and expand the benefits of immunotherapy.

MATERIALS AND METHODS

Mice and cell culture

C57BL/6J female mice, 6 weeks old, were purchased from Shanghai Lingchang Biotechnology. The animal study was reviewed and approved by the Institutional Animal Care and Use Committee of Shanghai Jiao Tong University School of Medicine (Approval number: A-2020–001). CTIAC11 cells were generously provided by the Rolf Brekken laboratory at the University of Texas Southwestern Medical Center. MC38, CT26, HEK293T, HT29, and Panc02 cells were obtained from the Cell Bank of the Shanghai Institutes for Biological Sciences, Chinese Academy of Sciences. All cells used in this study were tested to be free of Mycoplasma contamination.

Reagents and antibodies

The reagents used included luminespib (747412-49-3, Topscience); VER50589 (747413-08-7, Topscience); emricasan (254750-02-2, Topscience). Anti-PD-L1 antibody (Clone: 10F.9G2), anti-mouse CD8 antibody (Clone: 116–13.1), anti-mouse IFNAR-1 antibody (Clone: MARI-5A3) and isotype control were obtained from Bio X Cell. The fluorochrome-labeled anti-mouse antibodies used for flow cytometry were BV421-IFN- γ (505830; BioLegend); PerCP-Cy5.5-CD45 (103132; BioLegend); Fixable Viability Stain 780 (565388; BD Biosciences); CD8-APC (100712; BioLegend); CD4-V605 (562658; BD Pharmingen); TNF- α -PE (506306; BioLegend). The antibodies used for immunoblotting were anti-cGAS antibody (31659; CST); anti-STING antibody (13647; CST); anti-MAVS antibody (4983; CST); anti-MyD88 antibody (4283; CST); anti-GAPDH antibody (2118; CST); anti-Caspase-8 antibody (4790; CST); anti-Caspase-3 antibody (9662; CST); anti-Caspase-9 antibody (9504; CST); anti-Apaf-1 antibody (8969; CST); anti-Phospho-TBK1 antibody (5483; CST); anti-survivin antibody (2808; CST); anti-AIF antibody (5318; CST); anti-endonuclease G antibody (4969; CST); anti-tubulin antibody (5568; CST); anti- β -Actin antibody (3700; CST); anti-Bak antibody (3814; CST; 06–536, Sigma-Aldrich); anti-Bax antibody (2772; CST; Sc-23959, Santa Cruz); anti-Tom20 antibody (42406; CST); anti-Mcl-1 antibody (5453; CST); anti-Cleaved Caspase-9 antibody (9509; CST); anti-Cleaved Caspase-3 antibody (9661; CST); anti-PD-L1 (ab213480; Abcam). The anti-mouse antibodies used for immunohistochemistry were

anti-granzyme B antibody (44153; CST); anti-CD8 α antibody (44153; CST); anti-CD45 antibody (70257; CST). The anti-HSP70 antibody (10995-1-AP; Proteintech) was used for flow cytometry.

In vitro high-throughput drug screening

The commercial anticancer drug library was purchased from Topscience (L2100). RAW-Lucia interferon-stimulated gene (ISG) cells with an IRF-inducible Lucia luciferase reporter construct were acquired from InvivoGen. Raw-Lucia ISG cells were seeded at a density of 30,000 cells per well in a 96-well flat bottom plate (Corning). After adhering to the plate, Raw-Lucia ISG cells were treated with drugs (1 μ M) for 24 hours. Subsequently, 50 μ L supernatant was transferred to a 96-well opaque white plate, and 50 μ L QUANTI-Luc (InvivoGen) was added to detect luciferase activity.

CRISPR/Cas9-mediated gene knockout

Single guide RNAs (sgRNAs) were designed using the web-based tool CRISPR design (<http://crispr.mit.edu/>) and cloned into the vector lenti-CRISPR V.2 (Plasmid 49535, Addgene). The sgRNA targeting sequences are listed in online supplemental table 1.

In vivo tumor models

1×10^6 MC38 cells were injected subcutaneously into the flank of mice. For luminespib and emricasan treatment, luminespib and emricasan were dissolved in phosphate-buffered saline containing 10% Kolliphor EL (61791-12-6, SIGMA). Tumor-bearing mice were randomized and treated with luminespib (intraperitoneal injection, 75 mg/kg, every 2 days) and/or emricasan (intratumoral injection, 10 mg/kg, daily). Mice were killed when the tumor volume reached 2000 mm³. To block IFN- α / β receptor, tumor-bearing mice were injected intratumorally with anti-IFNAR1 antibody (150 μ g per mouse, every 3 days). To deplete CD8⁺ T cells, tumor-bearing mice were injected intraperitoneally with anti-mouse CD8 antibody (100 μ g per mouse, every 3 days). To block programmed death-ligand 1 (PD-L1) /programmed death-1 (PD-1) signaling pathway, tumor-bearing mice were injected intraperitoneally with anti-mouse PD-L1 antibody (100 μ g per mouse, every 4 days).

RNA extraction and quantitative real-time PCR

Total RNA from cells was extracted using the TRIzol Reagent (15596026, Invitrogen) and reverse-transcribed with the PrimeScript RT reagent Kit (RR047A, Takara). Real-time PCR was performed on an ABI7900HI (Applied Biosystems). Gene expression was normalized to β -actin or L32. The primer sequences are shown in online supplemental table 2.

siRNA-mediated gene silencing

For transfection of siRNAs, siRNAs were transfected into cells with Lipofectamine 3000 (Invitrogen) according to the manufacturer's protocol. After an additional 48

hours, cells were harvested for analysis. siRNA sequences were shown in online supplemental table 3.

Protein extraction and immunoblotting

Cells were lysed with RIPA buffer (PC101, Epizyme) supplemented with phosphatase (GRF102, Epizyme) and protease inhibitors (GRF101, Epizyme). Cytoplasmic and mitochondrial proteins were extracted following the manufacturer's instructions (C500051, Sangon Biotech). The protein samples were denatured using SDS-PAGE Sample Buffer (P0015F, Beyotime Biotechnology) by heating. Subsequently, protein samples were separated on 6%–15% PAGE gels, transferred to nitrocellulose membranes (Millipore), incubated with primary antibody overnight at 4°C and secondary antibodies for 2 hours at room temperature. Protein signals were detected with the Tanon Image Analysis System. To assess the activation of Bcl2-associated X and Bcl2 antagonist/killer (BAX and BAK), protein samples were incubated with anti-BAX 6A7 or anti-BAK 23–38 and then with Protein A/G agarose beads (Millipore). Beads were washed five times and proteins were denatured by heating for immunoblotting.

Transcriptomic analysis

MC38 cells were treated with indicated drugs for 24 hours. Total RNA was extracted for transcriptome sequencing. Sequencing libraries were generated using NEBNext Ultra RNA Library Prep Kit for Illumina (NEB, USA) following the manufacturer's recommendations. The resulting clean reads were mapped to the mouse reference genome sequence (GRCm39), and the expression matrix was obtained. To identify differentially expressed genes (DEGs), the R package "DEseq2" was used, with genes having an absolute log₂ fold change greater than 2 and false discovery rate (FDR) adjusted p value < 0.01 considered as DEGs. Gene enrichment analysis was performed using the Gene Set Enrichment Analysis (GSEA) software (V.4.3.2) and the gene set database of Molecular Signatures Database.

Statistical analysis

Statistical analysis was performed using R software (V.4.2.3), GSEA (V.4.3.2) or GraphPad Prism (V.9.0), and all experiments were repeated at least three times independently. All values were presented as the means \pm SEM. The statistical significance was examined through the Student's t-test, two-way ANOVA or log-rank test. A p value of < 0.05 was considered significant. Some related quantitative statistical analysis was also provided in online supplemental file 2.

RESULTS

Identification of Hsp90 inhibitor as an innate immune activator under caspase inhibition

To identify novel anticancer drugs with the potent potential to activate innate immunity, we first conducted a cell-based anticancer drug library screening approach using a well-established reporter system in RAW-Lucia ISG cells²⁹ (figure 1A). This reporter system is sensitive to murine type I IFNs and can be applied to assess the

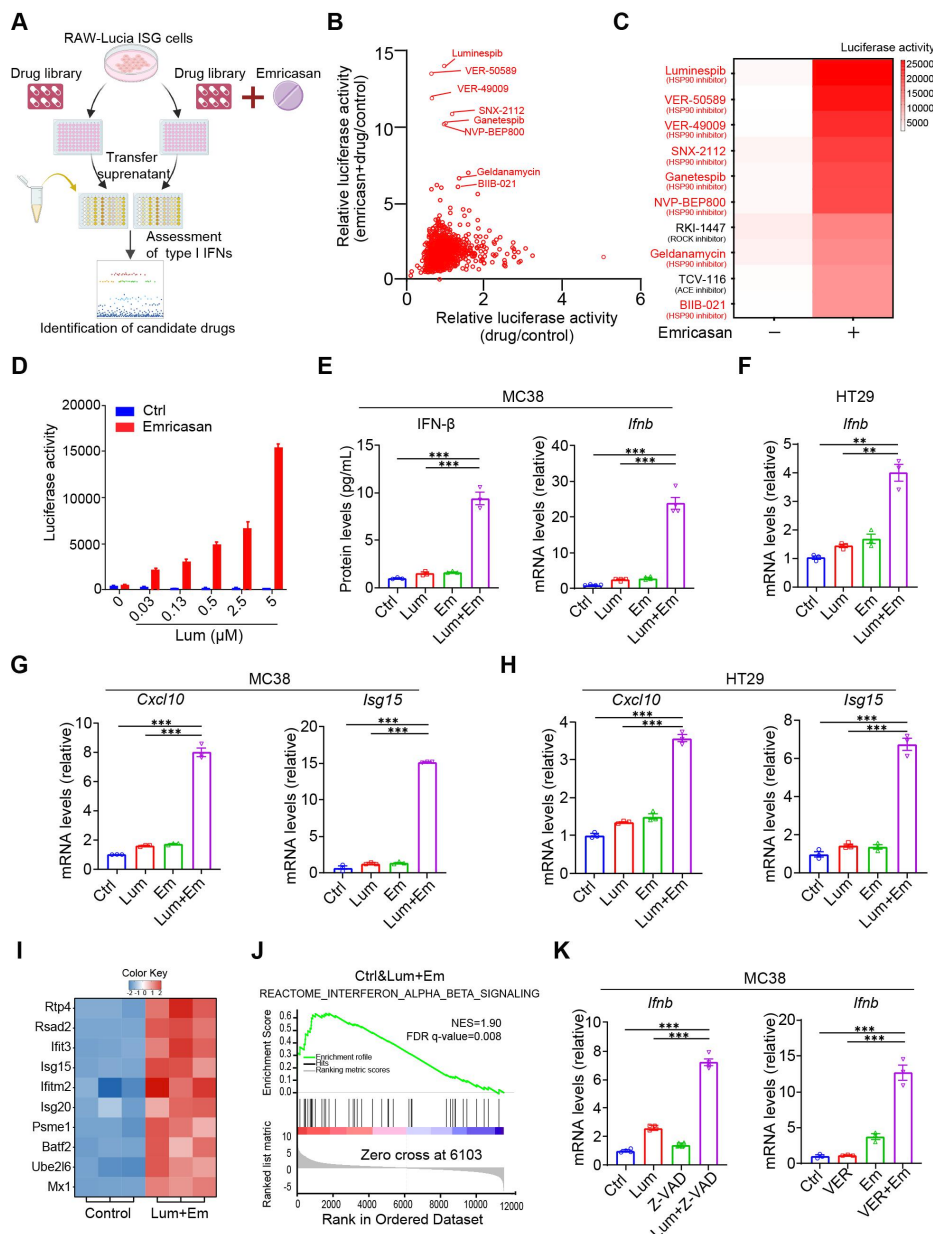


Figure 1 Caspase inhibition promotes Hsp90 inhibitor-induced tumor-intrinsic innate sensing. (A) Scheme of the in vitro high-throughput drug screen workflow. RAW-Lucia ISG cells were seeded in a 96-well flat bottom plate, and treated with each drug at a concentration of 1 μ M. After 24 hours, the supernatants were harvested and subsequently transferred to a 96-well opaque white plate. QUANTI-Luc substrate was added to detect the luciferase activity and assess the levels of type I IFNs. (B) The scatter plot showing the screening results normalized to control or emricasan. Hsp90 inhibitors were highlighted in red on the plot. (C) Heatmap based on luciferase activity showing the top 10 most significant compounds in the presence of emricasan. (D) RAW-Lucia ISG cells were planted in 96-well plates and treated with luminespib (Lum) \pm emricasan (Em, 10 μ M). After 24 hours, luciferase activity was assessed. (E) MC38 cells were treated with vehicle control (Ctrl), luminespib (Lum, 0.5 μ M), emricasan (Em, 10 μ M), luminespib and emricasan, respectively. After 24 hours, the supernatants were collected for IFN- β protein detection by ELISA (left); cells were collected for IFN- β detection by RT-qPCR (right). (F) HT29 cells were treated with vehicle control (Ctrl), luminespib (Lum, 0.5 μ M), emricasan (Em, 10 μ M), luminespib and emricasan, respectively. After 24 hours, cells were collected for IFN- β mRNA detection by RT-qPCR. (G, H) MC38 cells (G) and HT29 cells (H) were treated with indicated compounds for 24 hours. Cells were collected for Cxcl10 and Isg15 mRNA detection by RT-qPCR. (I) Heatmap showing the top 10 significantly enriched genes that belong to type I IFN signaling between the control and luminespib plus emricasan groups. The heatmap was made by calculating the Z-score values. (J) In MC38 cells, the activation changes of IFN- α/β signaling pathway in luminespib plus emricasan group compared with control group were revealed by GSEA. (K) MC38 cells were treated with indicated compounds for 24 hours. Cells were collected for the detection of IFN- β mRNA by RT-qPCR. The compounds used were Z-VAD-FMK (Z-VAD, 20 μ M), VER-50589 (VER, 2.5 μ M), luminespib (Lum, 0.5 μ M), and emricasan (Em, 10 μ M). Data are shown as mean \pm SEM ($n\geq 3$). P value was calculated by unpaired Student's t-test in (E–H and K). (** $p<0.01$, *** $p<0.001$). Hsp90, heat shock protein 90; IFN, interferon; ISG, interferon-stimulated gene; mRNA, messenger RNA; RT-qPCR, reverse transcription quantitative real-time PCR; GSEA, Gene Set Enrichment Analysis; FDR, false discovery rate.

drug's capability in inducing type I IFN production.^{30,31} One thousand two hundred and fourteen conventional chemotherapeutic and targeted antineoplastic drugs were included in this anticancer drug library. Notably, several well-known inducers of ICD, including tacedinaline,³² teniposide,³³ topotecan hydrochloride,³⁴ imatinib mesylate,³⁵ and epothilone B,³⁶ demonstrated the ability to promote type I IFN production (online supplemental table 4), thereby providing robust validation of the effectiveness of our screening system. Our results suggested that the addition of a caspase inhibitor emricasan, significantly improved the ability of screened drugs to induce the production of type I IFNs, particularly for drugs that do not inherently stimulate this response (figure 1B and online supplemental figure S1A). Importantly, emricasan alone did not exhibit effective type I IFN-generating activity, confirming its synergistic effect in our screening system.

Based on the screening results, we found that 8 of the top 10 candidate drugs were Hsp90 inhibitors (figure 1B,C and online supplemental figure S1A), which indicates the potent ability of Hsp90 inhibitors to stimulate type I IFN production. Notably, luminespib exhibited the most potent stimulatory effect on the production of type I IFNs (figure 1C), and its effect was dose-dependent (figure 1D and online supplemental figure S1B). We further confirmed the results in murine colorectal cancer cells MC38 and CT26, pancreatic cancer cells CTIAC11 and Panc02, and human colorectal cancer cell HT29. Luminespib or emricasan alone induced a marginal expression of IFN- β in all cell models (figure 1E,F and online supplemental figure S1C). However, combination treatment provoked a marked increase in IFN- β expression (figure 1E,F and online supplemental figure S1C), indicating synergistic effects between luminespib and emricasan. Consistently, the downstream signaling proteins (CXCL10 and ISG15) showed similar results (figure 1G,H, online supplemental figure S1D,E). Additionally, our transcriptomic (RNA sequencing) analysis also revealed a significant enrichment of type I IFN signaling after combination treatment (figure 1I,J and online supplemental figure S1F). To exclude any potential off-target effects of luminespib and emricasan, we tested another screened Hsp90 inhibitor VER50589, and another pan-caspase inhibitor Z-VAD-FMK, respectively. In line with the findings mentioned earlier, the combination of VER50589 and emricasan, as well as that of luminespib and Z-VAD-FMK, significantly enhanced the expression of IFN- β and its downstream signaling proteins (figure 1K, online supplemental figure S1G,H), confirming the role of Hsp90 and caspase in the process. Taken together, these results demonstrate that caspase inhibition promotes Hsp90-based chemotherapy-mediated type I IFN production.

Caspase inhibition promotes Hsp90 inhibitor-induced mtDNA release and triggers innate sensing through cGAS/STING pathway

To investigate the mechanistic basis of how luminespib in combination with caspase inhibitor activates type I IFNs, we first assessed the effects of combination treatment on the major steps of type I IFN signaling. Activation of cell-intrinsic type I IFNs is initiated by cytosolic nucleic acid sensing signaling,^{37,38} primarily via three distinct pathways (figure 2A): (1) sensing of cytosolic double-stranded DNA by cGAS; (2) sensing of cytosolic double-stranded RNA by retinoic acid-inducible gene I and melanoma differentiation-associated protein 5; (3) sensing of cytosolic single-stranded RNA by toll-like receptors. Notably, TANK-binding kinase 1 (TBK1) acts as a crucial signaling hub downstream of all three pathways, and is responsible for activating IRF3, leading to the production of type I IFNs and subsequent expression of ISGs. Our results showed that luminespib combined with caspase inhibitors (emricasan or Z-VAD-FMK) markedly activated TBK1 in MC38 and Panc02 cells (figure 2B and online supplemental figure S2A). Importantly, knockout of IRF3 abrogated the promoting effect of combination treatment on IFN- β production (figure 2C and online supplemental figure S2B), confirming the regulatory role of IRF3. To explore which upstream pathway is required for type I IFN production after combination treatment, we knocked out the key mediator of each signaling pathway in MC38 cells (online supplemental figure S2B). Similar to wild type, knockout of MyD88 or MAVS had minimal impact on IFN- β expression and TBK1 activation (figure 2C,D). In contrast, knockout of cGAS or STING showed similar results as knockout of IRF3, and largely diminished the activation of IFN- β and TBK1 induced by combination treatment (figure 2C,D). These results suggest that the combination treatment induces the production of type I IFNs via cGAS/STING/TBK1/IRF3 signaling.

Endogenous DNA sources that trigger STING activation include damaged genomic DNA (gDNA) and mtDNA.³⁹ Indeed, we observed that emricasan had no obvious effect on cytosolic DNA (figure 2E and online supplemental figure S2C), while luminespib significantly increased cytosolic DNA regardless of emricasan treatment (figure 2E and online supplemental figure S2C). The excessive cytosolic DNA induced by luminespib was mainly derived from the accumulation of gDNA and mtDNA (figure 2F,G). However, addition of emricasan reduced cytosolic gDNA levels but further promoted the mtDNA release compared with the group treated with luminespib alone (figure 2F,G). These results indicate that mtDNA may be the major DNA source for DNA sensing in combination treatment, and luminespib could function as an mtDNA inducer. To investigate whether mtDNA is required for the production of type I IFNs, we depleted mtDNA using dideoxycytidine (online supplemental figure S2D), and found that depletion of mtDNA dramatically abolished IFN- β production and TBK1 activation after combination treatment (figure 2H,I), thus confirming the involvement

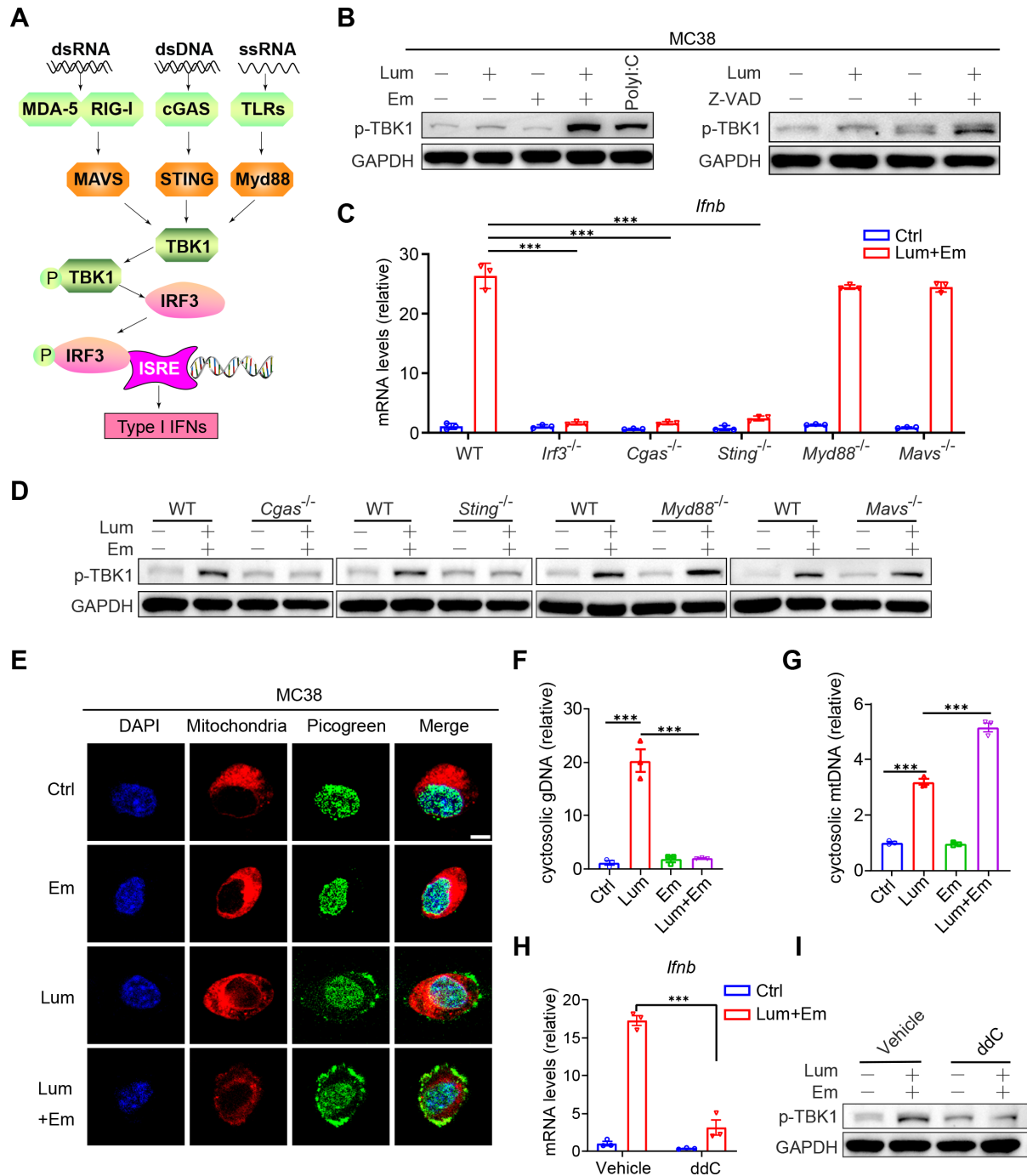


Figure 2 Hsp90 inhibitor combined with caspase inhibition promotes tumor-intrinsic mtDNA sensing. (A) Schematic diagram of the main pathways involved in intracellular production of type I interferons. (B) MC38 cells were treated with luminespib (Lum, 0.5 μ M) and emricasan (Em, 10 μ M) or Z-VAD-FMK (Z-VAD, 20 μ M) for 24 hours, the protein level of phosphorylated TBK1 (p-TBK1) was determined by western blot. Poly(I:C) (2 μ g/mL) was used as a positive control. (C, D) Indicated cells were treated with luminespib and emricasan for 24 hours. The mRNA expression of IFN- β was determined by RT-qPCR (C) and the protein level of p-TBK1 was determined by western blot (D). (E) Representative confocal images showing cytosolic DNA (PicoGreen, green), mitochondria (Mito-Tracker, red), and nuclei (DAPI, blue) in MC38 cells after indicated treatments. Scale bar, 5 μ m. (F, G) MC38 cells were treated with indicated compounds for 24 hours, cytosolic DNA was extracted, and the levels of gDNA (F) and mtDNA (G) were determined by RT-qPCR. (H, I) MC38 or ddC-treated MC38 (MC38-ddC) cells were treated with indicated compounds for 24 hours, and the mRNA expression of IFN- β was determined by RT-qPCR (H) and the protein level of p-TBK1 was determined by western blot (I). Data are shown as mean \pm SEM ($n \geq 3$). P value was calculated by unpaired Student's t-test in (C and F–H). (***) $p < 0.001$. RT-qPCR, reverse transcription quantitative real-time PCR; ddC, dideoxycytidine; dsDNA, double-stranded DNA; dsRNA, double-stranded RNA; ssRNA, single-stranded RNA; gDNA, genomic DNA; IFN, interferon; IRF3, interferon regulatory factor 3; MDA5, melanoma differentiation-associated protein 5; mRNA, messenger RNA; mtDNA, mitochondrial DNA; cGAS, the second messenger cyclic GMP-AMP; RIG-I, retinoic acid-inducible gene I; STING, stimulator of interferon gene; TBK1, TANK-binding kinase 1; TLR, toll-like receptor; WT, wild type.

of mtDNA in type I IFN production. Overall, these results demonstrate that inhibition of both Hsp90 and caspases induces mtDNA release, triggers cGAS/STING/TBK1/IRF3 pathways, and promotes the production of type I IFNs.

Blocking Caspase-9 signaling relieves the restriction of DNA sensing induced by Hsp90 inhibitor

MOMP is a crucial event that triggers mtDNA release into the cytosol. Previous studies have suggested that Hsp90 inhibitor can transcriptionally downregulate myeloid cell leukemia-1 (MCL-1),⁴⁰ an anti-MOMP protein that binds and inhibits the executioners of MOMP, including BAK and BAX.⁴¹ Therefore, we hypothesized that luminespib could induce MOMP by activating BAK and BAX, thus promoting mtDNA release. As expected, both luminespib alone and combination treatment significantly downregulated MCL-1 and upregulated BAK and BAX (figure 3A and online supplemental figure S3A). To further validate the activation of BAX and BAK, we employed conformation-specific antibodies targeting the activation epitope. Our results demonstrated significant activation of both BAK and BAX on treatment with the Hsp90 inhibitor alone, as well as in the combination treatment (figure 3A). Importantly, both luminespib alone and combination treatment stimulated the release of mitochondrial content, as evidenced by loss of mitochondrial cytochrome c expression and staining (figure 3B,C), thereby confirming the onset of MOMP. Furthermore, we observed a significant enrichment of the apoptosis pathway and an increase in the activity of Caspase-3/7 and the expression of cleaved Caspase-3 in luminespib-treated cells (figure 3D–F and online supplemental figure S3B). However, the activation of Caspase-3/7 was blocked by emricasan (figure 3E,F). Given that caspases can mediate the cleavage of cGAS/STING/TBK1, this could explain why luminespib induces the production of type I IFNs only in the presence of caspase inhibitor.

Emricasan is a pan-caspase inhibitor and blocks both intrinsic and extrinsic apoptosis. We next determined which apoptosis signaling is activated by luminespib. We knocked out Caspase-9 and Caspase-8 (online supplemental figure S3C), which are the key mediators of intrinsic and extrinsic apoptosis respectively, to mimic the function of emricasan. Similar to wild type, knockout of Caspase-8 failed to induce TBK1 activation as well as the expression of IFN- β and downstream signaling after luminespib treatment (figure 3G,H and online supplemental figure S3D). Conversely, deficiency of Caspase-9 exhibited similar effects to emricasan after luminespib treatment (figure 3G,H and online supplemental figure S3D), suggesting that Hsp90 inhibitor selectively activates Caspase-9 and subsequently mediates the restriction of type I IFN production. Indeed, we observed increased activity and a cleaved form of Caspase-9 following luminespib treatment (figure 3I,J). Moreover, we knocked out the upstream adapter protein APAF-1 and downstream executor Caspase-3 of Caspase-9 (online supplemental figure

S3C). We found that loss of both proteins led to TBK1 activation as well as the expression of IFN- β and downstream signaling after luminespib treatment (figure 3K,L and online supplemental figure S3E), further confirming the role of the intrinsic apoptosis in luminespib-induced type I IFNs. Above all, our results suggest that the Hsp90 inhibitor induces the activation of tumor-intrinsic Caspase-9 signaling, which in turn restricts the production of type I IFNs.

Blockade of Hsp90 and Caspase-9 induces caspase-independent cell death and enhances tumor immunogenicity

Although luminespib induces apoptosis, our RNA sequencing analysis showed that emricasan did not significantly impact the signaling pathways involved in the cell cycle and cell death following luminespib treatment (figure 4A), indicating that emricasan fails to prevent cell death. To validate our findings, we conducted experiments on both mouse and human cells, and found that emricasan did not reduce the cell death mediated by luminespib (figure 4B). Additionally, the levels of survivin, which is a client protein of Hsp90 and essential for cell survival, decreased following luminespib treatment, regardless of emricasan treatment (figure 4C). To further verify the role of Hsp90 in cell death, we tested another Hsp90 inhibitor, VER50589, and obtained similar results (online supplemental figure S4). These results suggest that caspase inhibition does not weaken the cytotoxicity of Hsp90 inhibitor, but instead shifts Hsp90 inhibitor-induced apoptosis towards caspase-independent cell death (CICD).

Apart from caspase-dependent apoptosis, MOMP can induce caspase-independent apoptosis by releasing other pro-apoptotic factors from the mitochondria, such as apoptosis-inducing factor (AIF) and endonuclease G.⁴² To investigate the role of AIF and endonuclease G in the combination treatment-induced cell death, we silenced their expression in MC38 cells using siRNA (figure 4D). However, knockdown of AIF or endonuclease G did not affect cell death following luminespib treatment regardless of emricasan treatment (figure 4D), ruling out the involvement of the two proteins. We next tested whether combination treatment induced other forms of CICD, such as necroptosis, ferroptosis or autophagy, using small molecular inhibitors. Strikingly, all tested inhibitors failed to reverse cell death (figure 4E), thus excluding the involvement of the three forms of CICD. During intrinsic apoptosis, MOMP disrupts mitochondrial function and, even in the absence of caspase activity, energy production eventually wanes and cells die.^{43,44} Therefore, luminespib-induced MOMP may activate a point-of-no-return cell death mechanism in the presence of emricasan, which may be responsible for the observed cell death.

ICD has emerged as a pivotal component of therapy-induced antitumor immunity.⁴⁵ To evaluate the ability of luminespib combined with emricasan to stimulate ICD of tumor cells, we investigated the fundamental molecular events of ICD in vitro, including the release of

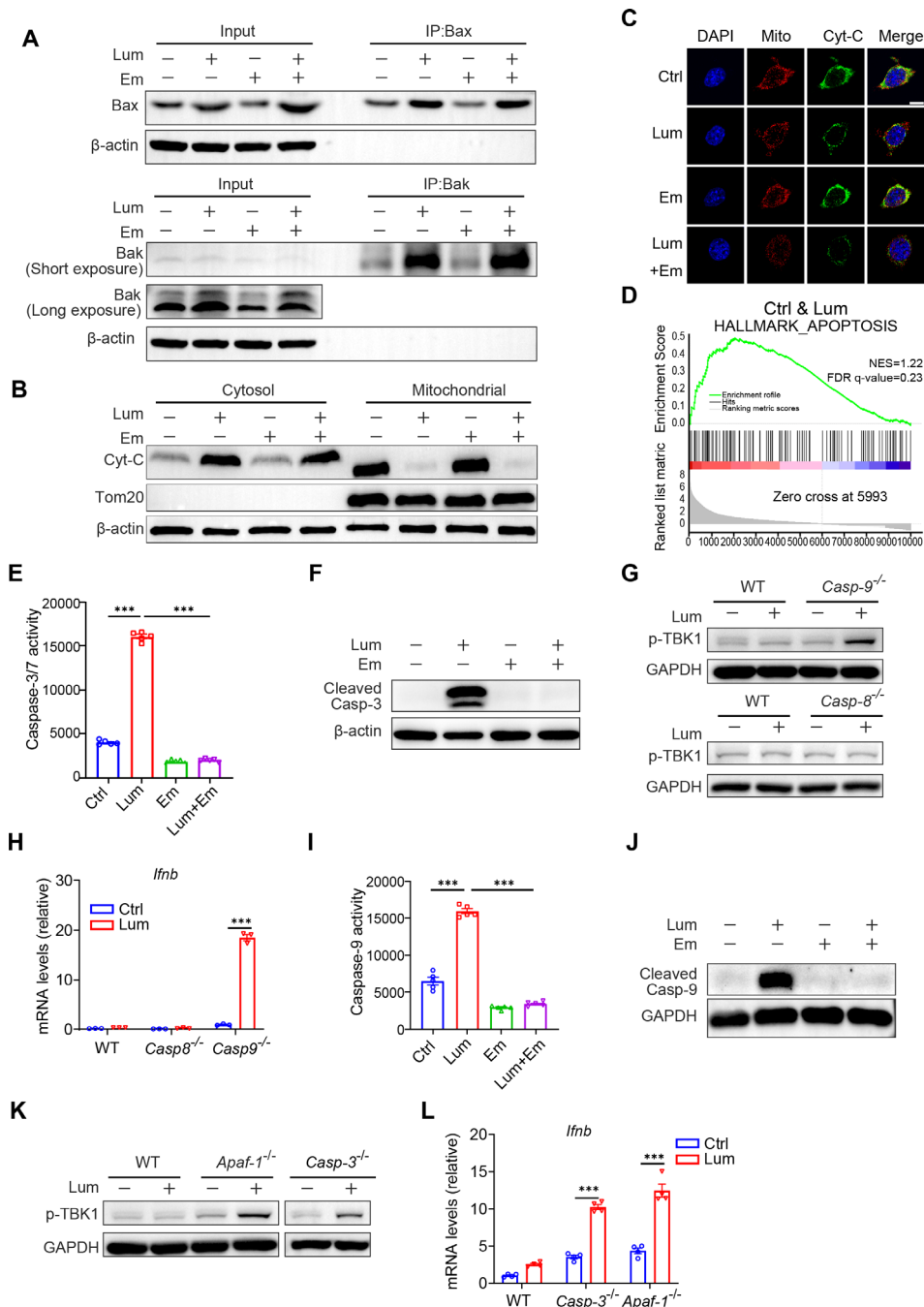


Figure 3 Tumor-intrinsic Caspase-9 signaling restricts Hsp90 inhibitor-mediated DNA sensing. (A) MC38 cells were treated with indicated treatments for 24 hours. The protein level of BAX and BAK was determined by western blot. The activation of BAX and BAK was analyzed by immunoprecipitation with the conformation-specific anti-Bax and anti-Bak antibodies. The Tom20 protein was used as a mitochondrial marker. (B) Cytochrome c (Cyt-C) was determined by western blot. (C) Representative confocal images showing Cyt-C (green), Tom-20/mitochondria (red), and nucleus (blue) in MC38 cells after indicated treatments. Scale bar, 10 μ m. (D) GSEA analysis revealing an upregulation of apoptosis signaling pathway in luminespib-treated group compared with control. (E, F) MC38 cells were treated with indicated compounds for 24 hours. The Caspase-3/7 activity was measured by Caspase-Glo 3/7 assay kit (E). The protein level of cleaved Caspase-3 was determined by western blot (F). (G, H) Indicated cells were treated with luminespib for 24 hours. The protein level of p-TBK1 was determined by western blot (G). The mRNA expression of IFN- β was determined by RT-qPCR (H). (I, J) MC38 cells were treated with indicated compounds for 24 hours. Caspase-9 activity was measured by Caspase-Glo 9 assay kit (I). The protein level of cleaved Caspase-9 was determined by western blot (J). (K, L) Indicated cells were treated with luminespib for 24 hours. The protein level of p-TBK1 was determined by western blot (K). The expression of IFN- β was determined by RT-qPCR (L). Data are shown as mean \pm SEM ($n \geq 3$). P value was calculated by unpaired Student's t-test in (E, H, I and L). (***) $p < 0.001$. BAK, Bcl2 antagonist/killer; BAX, Bcl2-associated X; IFN, interferon; mRNA, messenger RNA; NES, normalized enrichment score; GSEA, Gene Set Enrichment Analysis; FDR, false discovery rate; RT-qPCR, reverse transcription quantitative real-time PCR; TBK1, TANK-binding kinase 1; WT, wild type.

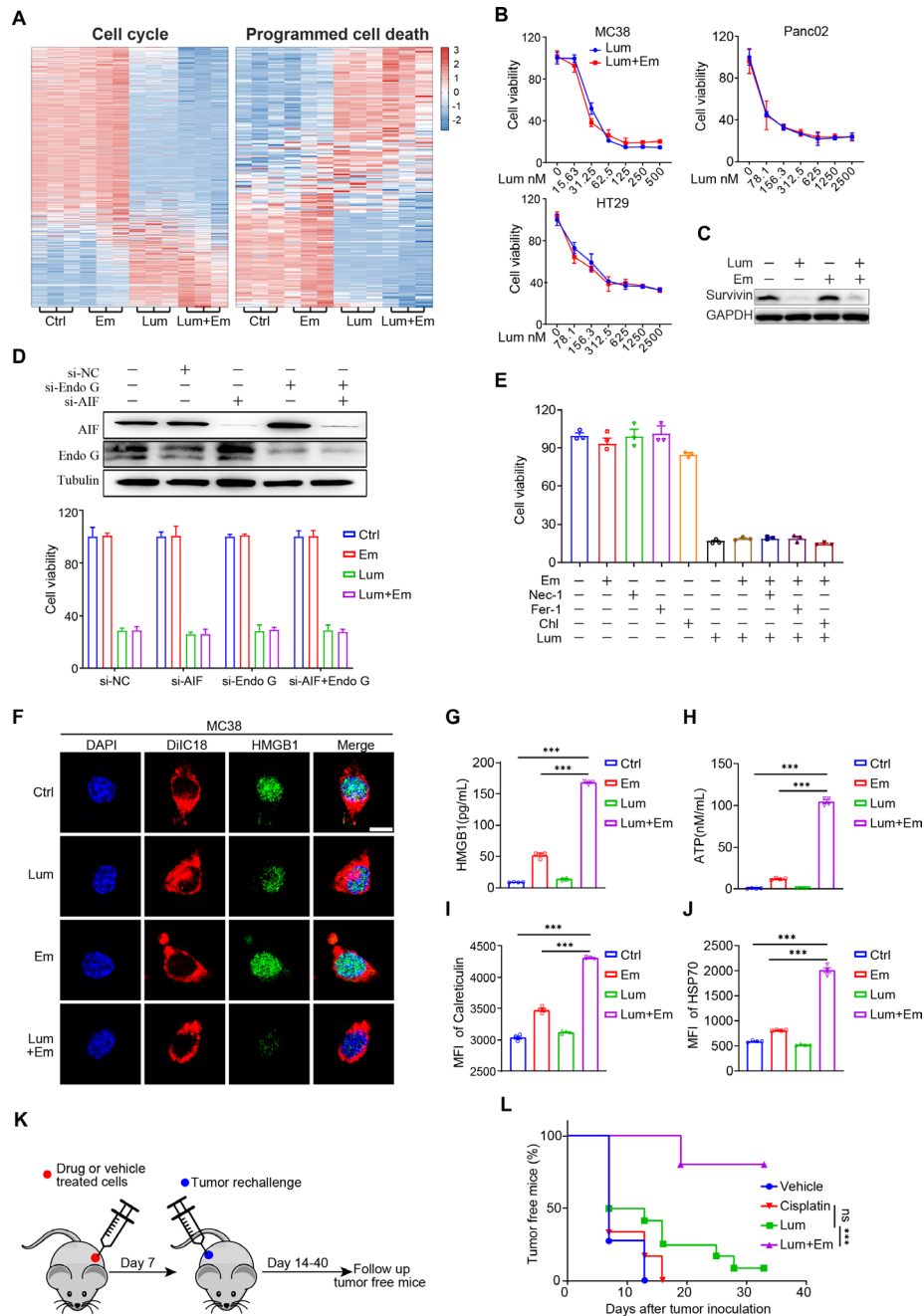


Figure 4 Targeting heat shock protein 90 and caspases induces caspase-independent cell death and enhances tumor immunogenicity. (A) Heat map showing the changes in cell cycle and programmed cell death signaling pathway in MC38 cells after indicated treatment. (B) MC38, Panc02, and HT29 cells were treated with luminespib (0–2.5 μ M) for 48 hours. Then cell viability was determined by Cell Counting Kit-8 (CCK-8) assay. (C) The protein level of survivin was determined by western blot. (D) MC38 cells were transfected with indicated siRNA, the efficiency of gene knockdown was detected by western blot and cell viability was determined by CCK-8 assay. (E) MC38 cells were treated with indicated compounds (Nec-1, necrostatin-1; Fer-1, ferrostatin-1; Chl, chloroquine) for 48 hours and cell viability was determined by CCK-8 assay. (F) Representative confocal images showing HMGB1 (green), DiIC18/cell membrane (red), and nucleus (blue) in MC38 cells after indicated treatments. Scale bar, 10 μ m. (G–J) MC38 cells were treated with indicated compounds for 24 hours. Then, the levels of HMGB1 (G) and ATP (H) released into the culture supernatant were quantified by an ELISA and an ATP test kit, respectively. Cells were harvested and cell surface expression of calreticulin (I) and Hsp70 (J) was measured by flow cytometry. (K) Scheme of in vivo tumor vaccination-rechallenge model. MC38-OVA cells were treated with lethal doses of luminespib, cisplatin, or combination of luminespib and emricasan in vitro, respectively. These treated cells were then inoculated subcutaneously into the flank of C57BL/6 mice. After 7 days, mice were rechallenged with live MC38-OVA cells by injection into the contralateral flank. (L) The percentage of rechallenged tumor-free mice was shown (tumor volume below 50 mm³ was recorded as tumor-free). Data are shown as mean \pm SEM ($n \geq 3$). P value was calculated by unpaired Student's t-test in (G–J) or log-rank test in (L). (ns, not significant, *** $p < 0.001$). AIF, apoptosis-inducing factor; HMGB1, high-mobility group box protein 1; MFI, Mean Fluorescence Intensity.

high-mobility group box protein 1 (HMGB1), the secretion of ATP, and surface exposure of calreticulin (CRT) and heat shock protein 70 (Hsp70). Our results showed that, unlike emricasan, luminespib alone promoted the secretion of HMGB1 and ATP, as well as the expression of CRT and Hsp70 on the cell surface (figure 4F–J), while combination with emricasan significantly magnified the promoting effects (figure 4F–J). To further validate the immunogenicity-inducing effect of combination treatment in vivo, we employed a classical tumor vaccination-rechallenge model in immunocompetent C57BL/6 mice. MC38 cells were pretreated with luminespib and emricasan to induce CICD. Cisplatin, an inefficient ICD inducer,⁴⁶ was used as a negative control. Dying cells were collected and injected as a vaccine into syngeneic mice. After 7 days, mice were rechallenged with live untreated MC38 cells on the opposite flank (figure 4K). As shown, immunization with luminespib-treated MC38 cells provided moderate protection against rechallenged tumor (figure 4L). However, mice immunized with combination-treated MC38 cells exhibited delayed tumor growth and 80% tumor-free survival (figure 4L). These results indicate that luminespib is insufficient to immunize mice and induce effective immunogenicity, but the combination with emricasan strengthens luminespib-mediated ICD-associated features and enhances specific antitumor immunogenicity.

Caspase-9 inhibition synergistically promotes Hsp90 inhibitor-mediated antitumor immunity

Type I IFN-mediated innate sensing and ICD-induced adaptive immunity are key elements in generating effective antitumor immune responses.^{6, 17} In light of this, we evaluated the antitumor efficacy of Hsp90 inhibitor combined with Caspase-9 inhibition in the syngeneic tumor model. MC38 cells were subcutaneously implanted into the right flank of mice, and luminespib was intraperitoneally injected once every 2 days. To minimize off-target side effects of emricasan and prime immune cells locally, emricasan was intratumorally administered every day for seven doses (online supplemental figure S5A). Both single treatments of luminespib or emricasan delayed tumor growth (figure 5A and online supplemental figure S5B). Notably, the combination treatment yielded more robust therapeutic effects with a tumor growth inhibition (TGI) rate of 71% (figure 5A and online supplemental figure S5B). Moreover, no obvious differences in body weight were observed among the groups (online supplemental figure S5C). We further validated the synergistic therapeutic efficacy in Caspase-9^{-/-} MC38 tumors. Similar to caspase inhibitor, loss of Caspase-9 also sensitized tumor to luminespib treatment (figure 5B and online supplemental figure S5D).

To validate the activation of type I IFN signaling in tumors, we analyzed the expression of IFN- β in TME following treatment. Either luminespib treatment or Caspase-9 inhibition did not alter the levels of IFN- β in tumors, but combination treatment dramatically

increased the production of IFN- β (figure 5C). To confirm the source of type I IFNs in vivo, we compared IFN- β expression between tumor (CD45⁻) and immune (CD45⁺) cells in the TME among treatment groups. The results demonstrated that it is Caspase-9^{-/-} tumor cells, rather than immune cells, that produce much more type I IFNs after luminespib treatment (figure 5D).

Type I IFN signaling plays an essential role in boosting cross-priming and CD8⁺ T-cell activation.⁴⁷ Indeed, only combination treatment exhibited a significant increase in the infiltration of immune cells (CD45⁺) and CD8⁺ T cells, along with the activation of CD8⁺ T cells [IFN- γ , tumor necrosis factor α (TNF- α) and granzyme-B] within the TME compared with single treatment groups (figure 5E,F, and online supplemental figure S6A–E), which corresponds to the potential of activating type I IFNs. To further investigate the activation of tumor-specific T-cell responses, we evaluated the tumor-reactivity of lymphocytes from the tumor-draining lymph nodes by co-culture with autologous-tumor cells in vitro. In contrast to the single treatment group, combination treatment enhanced the tumor-specific T-cell response (figure 5G). Additionally, the intratumoral level of IFN- γ was also markedly elevated on combination treatment (figure 5H). These results suggest that combination treatment stimulates a robust adaptive antitumor immune response.

In order to address the role of type I IFN signaling in antitumor effect, we blocked IFN- α/β receptor with anti-IFN- α R1 antibody (figure 5I). Remarkably, blockade of type I IFN signaling completely abolished the therapeutic effect of combination treatment (figure 5J). To further determine the involvement of CD8⁺ T cells in limiting tumor growth, we depleted CD8⁺ T cells through anti-CD8 antibody (figure 5I). After depletion of CD8⁺ T cells, combination treatment was no longer able to control tumor growth (figure 5J). These results suggest that both type I IFN signaling and CD8⁺ T cells are required for combination treatment-mediated tumor regression. Collectively, our results demonstrate that Caspase-9 inhibition in tumor cells can improve Hsp90 inhibitor-mediated antitumor immune responses by activating innate sensing and tumor-specific T-cell immunity.

Targeting Hsp90 and Caspase-9 synergizes with immunotherapy to overcome immune evasion and improve systemic antitumor response

Immune evasion poses a considerable challenge in fully realizing the clinical potential of immunotherapies, and the PD-1/PD-L1 immunoinhibitory axis represents a common mechanism for evading immune surveillance.⁴⁸ Given that PD-L1 is an inducible gene regulated by type I IFNs, we investigated whether PD-1/PD-L1 signaling exists in tumor and impedes antitumor immune responses following combination treatment. We first analyzed PD-L1 expression on tumor cells and found that combination treatment significantly increased the expression of PD-L1 at both mRNA and protein levels (figure 6A,B), as well as on the cell membrane of tumor

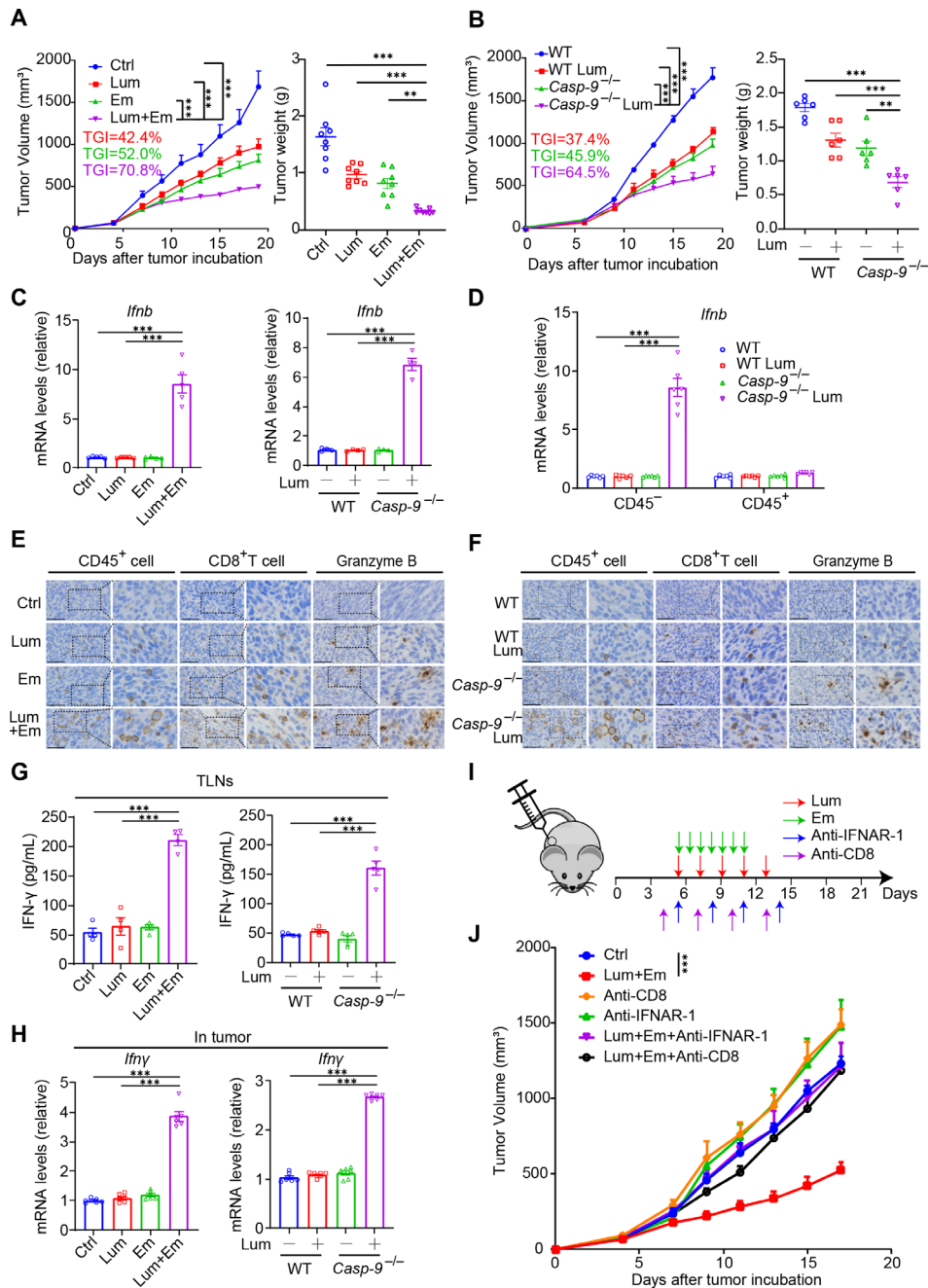


Figure 5 Targeting Hsp90 and Caspase-9 suppresses tumor growth by activating type I IFN signaling and T-cell immunity. (A) C57BL/6 mice ($n=8$ per group) were transplanted with 1×10^6 MC38 cells and subjected to treatment with luminespib (75 mg/kg, every 2 days for a total of five times) and/or emricasan (10 mg/kg, daily for 7 days). Tumor growth was monitored (left) and tumor weights (right) were measured when mice were euthanized. (B) C57BL/6 mice ($n=6$ per group) were transplanted with 1×10^6 wild type (WT) or Caspase-9-deficient (*Casp9*^{-/-}) MC38 cells and then treated with luminespib every 2 days. Tumor growth was monitored (left) and tumor weights (right) were measured when mice were euthanized. (C) After indicated treatments, the mRNA expression of IFN- β in tumor tissues was determined by RT-qPCR. (D) The mRNA expression of IFN- β in live tumor cells (CD45⁻) and immune cells (CD45⁺) isolated from tumor tissues was determined by RT-qPCR. (E) Immunohistochemistry showing the proportion of tumor-infiltrating immune cells and CD8⁺ T cells as well as the expression of granzyme B in MC38 tumors after indicated treatments. Scale bar, 50 μ m. (F) Immunohistochemistry showing the proportion of tumor-infiltrating immune cells and CD8⁺ T cells as well as the expression of granzyme B in WT or *Casp9*^{-/-} MC38 tumors after indicated treatments. Scale bar, 50 μ m. (G) Single-cell suspensions were isolated from tumor drain lymph nodes (TLNs) of tumor-bearing mice, and re-stimulated with dead MC38 cells for 48 hours. The level of IFN- γ in cultural supernatant was quantified by ELISA. (H) After indicated treatments, the mRNA expression of IFN- γ in tumor tissues was determined by RT-qPCR. (I) Scheme of in vivo T-cell depletion and blockade of type I IFN signaling experiments. (J) C57BL/6J mice ($n=7$) were transplanted with 1×10^6 MC38 cells. After indicated treatments, tumor growth was monitored. Data are shown as mean \pm SEM. P value was calculated by unpaired Student's t-test in (A–D, G and H) or two-way ANOVA analysis of variance in (A, B and J). (** $p < 0.01$, *** $p < 0.001$). TGI, tumor growth inhibition; RT-qPCR, reverse transcription quantitative real-time PCR; IFN, interferon; mRNA, messenger RNA.

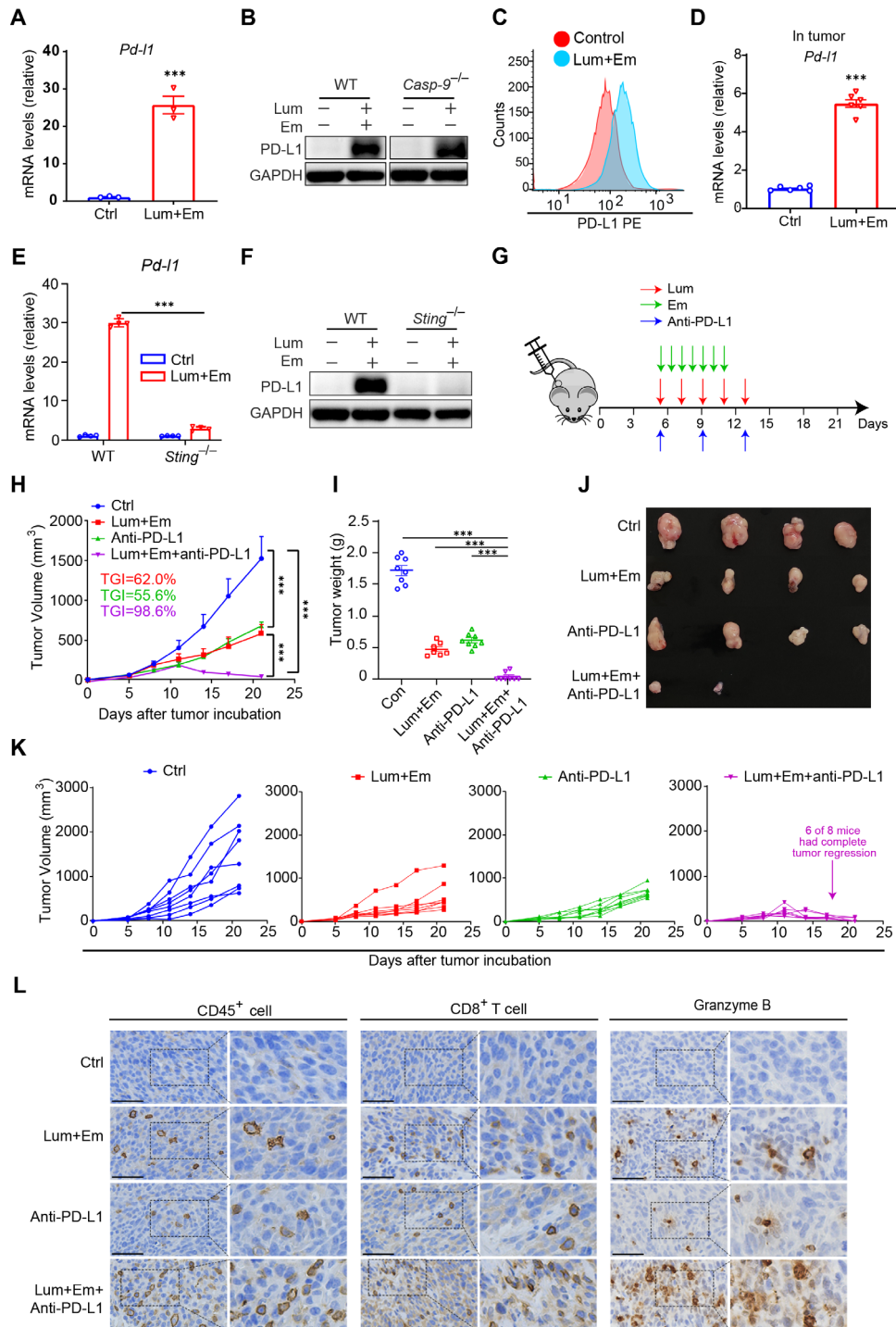


Figure 6 Heat shock protein 90 inhibitor synergizes with caspase inhibition and PD-L1 blockade to overcome adaptive resistance and render tumors eradicable. (A–C) MC38 cells were treated with luminespib and emricasan for 24 hours. The mRNA expression of PD-L1 was determined by RT-qPCR (A), the protein level of PD-L1 was determined by western blot (B) and the cell surface expression of PD-L1 was determined by flow cytometry (C). (D) The mRNA expression of PD-L1 in tumor tissues after treatment with luminespib and emricasan was determined by RT-qPCR. (E, F) WT or *Sting*^{-/-} MC38 cells were treated with luminespib and emricasan for 24 hours. The mRNA expression of PD-L1 was determined by RT-qPCR (E) and the protein level of PD-L1 was determined by western blot (F). (G) Scheme of tumor triple-therapy model in C57BL/6J mice. (H, I) After indicated treatments, tumor growth was monitored (H) and tumor weights were measured when mice were euthanized (I). (J) Representative photographs of MC38 tumors after indicated treatments. (K) Tumor growth curves of individual mice in (H) for visibility. (L) Immunohistochemistry showing the proportion of tumor-infiltrating immune cells and CD8⁺ T cells as well as the expression of granzyme B in MC38 tumors after indicated treatments. Scale bar, 50 μ m. Data are shown as mean \pm SEM ($n \geq 3$). P value was calculated by unpaired Student's t-test in (A, D, E and I) or two-way ANOVA analysis of variance in (H). (***) $p < 0.001$. RT-qPCR, reverse transcription quantitative real-time PCR; mRNA, messenger RNA; PD-L1, programmed death-ligand 1; STING, stimulator of interferon genes; WT, wild type.

cells (figure 6C), where PD-L1 exerts its function. Moreover, upregulated PD-L1 expression was also observed in tumor tissues under the combination with luminespib and emricasan treatment (figure 6D). Next, we explored whether type I IFN signaling is required for the upregulation of PD-L1 expression. We found that the upregulation of PD-L1 mediated by combination treatment was almost completely abolished in STING-deficient MC38 cells (figure 6E,F), thus confirming its dependence on type I IFN signaling.

To evaluate the impact of PD-L1 upregulation on immune suppression, we treated MC38 tumor-bearing mice with anti-PD-L1 antibody (figure 6G). Our results showed that PD-L1 blockade alone had a moderate inhibition on tumor growth, while the triple combination treatment produced the best therapeutic outcome (figure 6H–K), with 75% of tumors completely rejected. This robust synergistic effect was associated with enhanced infiltration of CD45⁺ and CD8⁺ T cells, as well as the activation of CD8⁺ T cells in tumor tissues (figure 6L), indicating effective reactivation of T-cell immunity. Considering that MC38 cells are sensitive to anti-PD-1/PD-L1 therapy, we expanded our evaluation to an anti-PD-L1-resistant tumor model using B16 cells. Similar to our observations in the MC38 tumor model, the combination treatment also sensitized B16 tumors to PD-L1 blockade (online supplemental figure S7), highlighting the potential of our combination approach to enhance the efficacy of immunotherapy, even in immunotherapy-resistant tumor models.

To determine whether the local delivery of emricasan could trigger systemic antitumor responses, MC38 cells were subcutaneously injected into both the left flank as the primary tumor and the right flank as the distant tumor. In this experimental set-up, the primary tumor received intratumoral injection of emricasan along with intraperitoneal injections of luminespib and α PD-L1, while the distant tumor remained untreated. Our results revealed that either α PD-L1 alone or the dual combination treatment significantly delayed the growth of both primary and distant tumors, but the triple combination treatment had the most substantial effect (online supplemental figure S8). Notably, distant tumors in all treatment groups were larger compared with the primary tumors (online supplemental figure S8). We speculate that emricasan, in addition to its inherent antitumor effects, may provide stronger innate and adaptive immune activation at the local tumor site compared with the distant site, possibly through caspase inhibition.

Given that emricasan is an orally pan-caspase inhibitor in clinical trials, we also investigated its potential therapeutic effects through systemic administration. We observed that, regardless of the route of emricasan administration (oral, intraperitoneal, or intratumoral), the combination treatment significantly reduced tumor growth (online supplemental figure S9). Moreover, these effects were further enhanced when combined with anti-PD-L1 therapy. It is worth noting that intratumoral

emricasan administration in both dual and triple combinations yielded the most remarkable therapeutic effects (online supplemental figure S9), possibly due to the notion that it provided the strongest caspase inhibition at the tumor site.

Taken together, our findings suggest that targeting Hsp90 and Caspase-9 induces adaptive immune evasion by upregulating PD-L1, while PD-L1 blockade provokes a potent synergy and potentiates the therapeutic efficacy. This rational triple combination treatment not only achieves impressive local tumor control but also induces a robust systemic antitumor response.

DISCUSSION

Traditional cancer therapies, such as chemotherapy, radiotherapy and targeted therapy, primarily focus on the direct destruction of cancer cells, with minimal attention to the key role of innate immunity in cancer progression. As a result, their clinical efficacy is often limited. To address this issue, we proposed that caspase inhibition could alleviate the intrinsic inhibitory signaling of innate sensing and enhance the antitumor immunity of anticancer agents. In this study, we screened an anticancer drug library and identified Hsp90 inhibitor as a potent agent potentially improving innate sensing. Under caspase inhibition, Hsp90 inhibitor exhibited impressive antitumor effects *in vivo*, primarily relying on the activation of innate and adaptive immunity. Importantly, this rational combination treatment showed a remarkable synergistic therapeutic effect with anti-PD-L1 therapy, which resulted in complete tumor regression in 75% of cases.

Hsp90 is a conserved molecular chaperone that is usually overexpressed in tumor cells.^{49,50} By regulating the stability and activation of over 200 client proteins, Hsp90 plays prominent functional roles in regulating a variety of cellular processes.⁵⁰ While Hsp90 inhibitors primarily exhibit antitumor effects through cytotoxicity on tumor cells,⁵¹ their potential impact on antitumor immunity cannot be overlooked due to the role of Hsp90 in immunomodulation.⁵² In our experimental systems, Hsp90 inhibitors constituted 8 out of the top 10 candidate anticancer drugs, thus indicating their potent capacity to modulate the innate immune response. Notably, although Hsp90 inhibitor alone only induced a slight production of type I IFNs, this effect was greatly enhanced under caspase inhibition in a cGAS/STING-dependent manner, thereby confirming a synergistic effect rather than a direct activation of innate sensing. Mechanically, Hsp90 inhibitor was able to induce MOMP and mtDNA release, which can trigger STING-mediated innate sensing. However, MOMP also resulted in cytochrome c release, which subsequently triggered caspase activation and mediated cGAS/TBK1/STING cleavage, thus suppressing innate sensing. This partially explains the limited efficacy of Hsp90 inhibitors observed in clinical trials.



Although Hsp90 inhibitor can induce apoptosis, caspase inhibitor emricasan did not alleviate Hsp90 inhibitor-mediated cytotoxicity, suggesting that this combination would not reduce the antitumor effect of Hsp90 inhibitor itself. Also, caspase inhibition shifted Hsp90 inhibitor-induced apoptosis towards CICD. However, several conventional inhibitors of CICD failed to reverse the cell death induced by combination treatment, suggesting that a specific form of CICD may need to be further explored. One of the main drawbacks of traditional chemotherapy drugs is their lack of specificity, which can result in adverse toxicity to non-targeted tissues, including the immune cells.⁵³ In our *in vivo* studies, we did not observe differences in body weight and impairment of immune cells and CD8⁺ T cells in the setting of single or combination treatment. In contrast, combination treatment significantly increased the infiltration of immune cells and established a T cell-inflamed TME, thus excluding the adverse toxicity of combination treatment on the immune system. ICD, an inflammatory form of cell death, involves the release of endogenous danger signals from dying tumor cells, which promote the recruitment, activation, and maturation of dendritic cells, thereby facilitating the priming of T cells and activating a tumor-specific immune response.⁵⁴ Our results showed that caspase inhibition could enhance Hsp90 inhibitor-induced ICD and prevent tumor rechallenge, suggesting that combination treatment also activates adaptive immunity and triggers innate sensing. Despite a previous study has reported that Hsp90 inhibitors can suppress tumor immunogenicity mediated by surface Hsp90, our research results suggested that the release of other damage-associated molecular patterns induced by the combination treatment may play a more significant role in this process.

Reducing tumor burden, enhancing immunogenicity, and activating innate immunity are considered effective strategies to improve immunotherapy.⁵⁵ Our results showed that co-inhibition of Hsp90 and caspase could effectively activate the three critical pathways simultaneously, highlighting the potential of this approach as a promising candidate for combination with immunotherapy. Of note, the combination of Hsp90 and caspase inhibitors induced an adaptive immune evasion by regulating PD-L1, which limited its antitumor efficacy. However, this limitation was overcome by the combination with anti-PD-L1 immunotherapy. This powerful synergistic effect led to complete tumor regression and triggered robust systemic antitumor responses.

In conclusion, this work highlights the potential of caspase inhibition in enhancing the antitumor immune response of anticancer drugs, and identifies the Hsp90 inhibitor as a potent innate immune adjuvant. Along with its direct cytotoxic effects on tumor cells, Hsp90 inhibitors can activate both innate and adaptive immunity under caspase inhibition, leading to remarkable antitumor effects. Importantly, the combination of anti-PD-L1 immunotherapy with Hsp90 inhibitor and caspase inhibitor was shown to achieve tumor regression

and induce systemic antitumor responses, providing a promising strategy for cancer therapy. These findings provide rationale and preclinical evidence for the potential clinical application of Hsp90 inhibitors in cancer treatment.

Contributors JL, XH and MS contributed equally to this paper. JL, XH, MS conceived the study. JL, XH, MS, WL, GY, HC, BG and JL contributed to acquisition of data. JL, MS, XH and XL analyzed the data. XH performed transcriptomic analysis. JL, MS and XL drafted the manuscript. XL and HW revised the manuscript. XL and HW supervised the study and responsible for the overall content as guarantors.

Funding This study was supported by grants from the National Natural Science Foundation of China (81972820 and 82030099), the National Key R&D Program of China (2018YFC2000700 and 2022YFD2101500), the Science and Technology Commission of Shanghai Municipality (22DZ2303000), Natural Science Foundation of Shanghai (23ZR1435900), Innovative research team of high-level local universities in Shanghai and Shanghai Jiao Tong University Key Program of Medical Engineering (YG2021ZD01).

Competing interests None declared.

Patient consent for publication Not applicable.

Ethics approval Not applicable.

Provenance and peer review Not commissioned; externally peer reviewed.

Data availability statement All data relevant to the study are included in the article or uploaded as supplementary information.

Supplemental material This content has been supplied by the author(s). It has not been vetted by BMJ Publishing Group Limited (BMJ) and may not have been peer-reviewed. Any opinions or recommendations discussed are solely those of the author(s) and are not endorsed by BMJ. BMJ disclaims all liability and responsibility arising from any reliance placed on the content. Where the content includes any translated material, BMJ does not warrant the accuracy and reliability of the translations (including but not limited to local regulations, clinical guidelines, terminology, drug names and drug dosages), and is not responsible for any error and/or omissions arising from translation and adaptation or otherwise.

Open access This is an open access article distributed in accordance with the Creative Commons Attribution Non Commercial (CC BY-NC 4.0) license, which permits others to distribute, remix, adapt, build upon this work non-commercially, and license their derivative works on different terms, provided the original work is properly cited, appropriate credit is given, any changes made indicated, and the use is non-commercial. See <http://creativecommons.org/licenses/by-nc/4.0/>.

ORCID iDs

Xiaoguang Li <http://orcid.org/0000-0002-2362-9130>

Hui Wang <http://orcid.org/0000-0003-2791-8981>

REFERENCES

- Sharma P, Hu-Lieskovan S, Wargo JA, *et al*. Primary, adaptive, and acquired resistance to cancer immunotherapy. *Cell* 2017;168:707–23.
- Gonzalez H, Hagerling C, Werb Z. Roles of the immune system in cancer: from tumor initiation to metastatic progression. *Genes Dev* 2018;32:1267–84.
- Bonaventura P, Shekarian T, Alcazer V, *et al*. Cold tumors: a therapeutic challenge for immunotherapy. *Front Immunol* 2019;10:168.
- Mahoney KM, Rennert PD, Freeman GJ. Combination cancer immunotherapy and new immunomodulatory targets. *Nat Rev Drug Discov* 2015;14:561–84.
- Woo SR, Corrales L, Gajewski TF. The STING pathway and the T cell-inflamed tumor microenvironment. *Trends Immunol* 2015;36:250–6.
- Corrales L, Matson V, Flood B, *et al*. Innate immune signaling and regulation in cancer immunotherapy. *Cell Res* 2017;27:96–108.
- Zitvogel L, Galluzzi L, Kepp O, *et al*. Type I Interferons in anticancer immunity. *Nat Rev Immunol* 2015;15:405–14.
- Yu R, Zhu B, Chen D. Type I interferon-mediated tumor immunity and its role in immunotherapy. *Cell Mol Life Sci* 2022;79:191.
- Bald T, Landsberg J, Lopez-Ramos D, *et al*. Immune cell-poor melanomas benefit from PD-1 blockade after targeted type I IFN activation. *Cancer Discov* 2014;4:674–87.

- 10 Morimoto Y, Kishida T, Kotani SI, *et al.* Interferon-beta signal may up-regulate PD-L1 expression through IRF9-dependent and independent pathways in lung cancer cells. *Biochem Biophys Res Commun* 2018;507:330–6.
- 11 Sumida TS, Dulberg S, Schupp JC, *et al.* Type I interferon transcriptional network regulates expression of coinhibitory receptors in human T cells. *Nat Immunol* 2022;23:632–42.
- 12 Xia T, Konno H, Ahn J, *et al.* Deregulation of STING signaling in colorectal carcinoma constrains DNA damage responses and correlates with tumorigenesis. *Cell Rep* 2016;14:282–97.
- 13 Zhang Y, Zhai Q, Feng X, *et al.* Cancer cell-intrinsic STING is associated with CD8 + T-cell infiltration and might serve as a potential Immunotherapeutic target in hepatocellular carcinoma. *Clin Transl Oncol* 2021;23:1314–24.
- 14 Corrales L, McWhirter SM, Dubensky TW, *et al.* The host STING pathway at the interface of cancer and immunity. *J Clin Invest* 2016;126:2404–11.
- 15 Khoo LT, Chen LY. Role of the cGAS-STING pathway in cancer development and oncotherapeutic approaches. *EMBO Rep* 2018;19:e46935.
- 16 Heinhuis KM, Ros W, Kok M, *et al.* Enhancing antitumor response by combining immune checkpoint inhibitors with chemotherapy in solid tumors. *Ann Oncol* 2019;30:219–35.
- 17 Ahmed A, Tait SWG. Targeting immunogenic cell death in cancer. *Mol Oncol* 2020;14:2994–3006.
- 18 Kroemer G, Galassi C, Zitvogel L, *et al.* Immunogenic cell stress and death. *Nat Immunol* 2022;23:487–500.
- 19 Fogarty CE, Bergmann A. The sound of silence: signaling by apoptotic cells. *Curr Top Dev Biol* 2015;114:241–65.
- 20 Nagata S, Tanaka M. Programmed cell death and the immune system. *Nat Rev Immunol* 2017;17:333–40.
- 21 Carneiro BA, El-Deiry WS. Targeting apoptosis in cancer therapy. *Nat Rev Clin Oncol* 2020;17:395–417.
- 22 Cao X, Wen P, Fu Y, *et al.* Radiation induces apoptosis primarily through the intrinsic pathway in mammalian cells. *Cell Signal* 2019;62:109337.
- 23 Ning X, Wang Y, Jing M, *et al.* Apoptotic caspases suppress type I interferon production via the cleavage of cGAS, MAVS, and IRF3. *Mol Cell* 2019;74:19–31.
- 24 Rongvaux A, Jackson R, Harman CCD, *et al.* Apoptotic caspases prevent the induction of type I interferons by mitochondrial DNA. *Cell* 2014;159:1563–77.
- 25 Xiong Y, Tang YD, Zheng C. The crosstalk between the caspase family and the cGAS–STING signaling pathway. *J Mol Cell Biol* 2021;13:739–47.
- 26 McArthur K, Kile BT. Apoptotic mitochondria prime anti-tumour immunity. *Cell Death Discov* 2020;6:98.
- 27 Han C, Liu Z, Zhang Y, *et al.* Tumor cells suppress radiation-induced immunity by hijacking caspase 9 signaling. *Nat Immunol* 2020;21:546–54.
- 28 White MJ, McArthur K, Metcalf D, *et al.* Apoptotic Caspases suppress mtDNA-induced STING-mediated type I IFN production. *Cell* 2014;159:1549–62.
- 29 Xie Z, Wang Z, Fan F, *et al.* Structural insights into a shared mechanism of human STING activation by a potent agonist and an autoimmune disease-associated Mutation. *Cell Discov* 2022;8:133.
- 30 Lama L, Adura C, Xie W, *et al.* Development of human cGAS-specific small-molecule inhibitors for repression of dsDNA-triggered interferon expression. *Nat Commun* 2019;10:2261.
- 31 Wu Y-T, Fang Y, Wei Q, *et al.* Tumor-targeted delivery of a STING agonist improves cancer immunotherapy. *Proc Natl Acad Sci U S A* 2022;119:e2214278119.
- 32 Marquardt V, Theruvath J, Pauck D, *et al.* Tacedinaline (CI-994), a class I HDAC inhibitor, targets intrinsic tumor growth and leptomeningeal dissemination in MYC-driven Medulloblastoma while making them susceptible to anti-Cd47-induced macrophage Phagocytosis via NF-kB-TGM2 driven tumor inflammation. *J Immunother Cancer* 2023;11:e005871.
- 33 Wang Z, Chen J, Hu J, *et al.* cGAS/STING axis mediates a topoisomerase II inhibitor-induced tumor immunogenicity. *J Clin Invest* 2019;129:4850–62.
- 34 Huang KC-Y, Chiang S-F, Yang P-C, *et al.* Immunogenic cell death by the novel topoisomerase I inhibitor TLC388 enhances the therapeutic efficacy of radiotherapy. *Cancers* 2021;13:1218.
- 35 Zitvogel L, Rusakiewicz S, Routy B, *et al.* Immunological off-target effects of Imatinib. *Nat Rev Clin Oncol* 2016;13:431–46.
- 36 Vacchelli E, Senovilla L, Eggermont A, *et al.* Trial watch: chemotherapy with immunogenic cell death Inducers. *Oncotarget* 2013;2:e23510.
- 37 Soppel N, Pflaum A, Kölle J, *et al.* The unresolved role of interferon-Lambda in asthma bronchiale. *Front Immunol* 2017;8:989.
- 38 Ghosh Z, Nakhhae M, Samie M, *et al.* Innate immune sensors for detecting nucleic acids during infection. *Journal of Laboratory Medicine* 2022;46:155–64.
- 39 Smith JA. STING, the endoplasmic reticulum, and mitochondria: is three a crowd or a conversation? *Front Immunol* 2020;11:611347.
- 40 Busacca S, Law EWP, Powley IR, *et al.* Resistance to HSP90 inhibition involving loss of MCL1 addiction. *Oncogene* 2016;35:1483–92.
- 41 Renault TT, Floros KV, Elkholi R, *et al.* Mitochondrial shape governs BAX-induced membrane permeabilization and apoptosis. *Mol Cell* 2015;57:69–82.
- 42 Chipuk JE, Bouchier-Hayes L, Green DR. Mitochondrial outer membrane permeabilization during apoptosis: the innocent bystander scenario. *Cell Death Differ* 2006;13:1396–402.
- 43 Ricci JE, Waterhouse N, Green DR. Mitochondrial functions during cell death, a complex (I-V) dilemma. *Cell Death Differ* 2003;10:488–92.
- 44 Lopez J, Tait SWG. Mitochondrial apoptosis: killing cancer using the enemy within. *Br J Cancer* 2015;112:957–62.
- 45 Galluzzi L, Buqué A, Kepp O, *et al.* Immunogenic cell death in cancer and infectious disease. *Nat Rev Immunol* 2017;17:97–111.
- 46 Martins I, Kepp O, Schlemmer F, *et al.* Restoration of the immunogenicity of cisplatin-induced cancer cell death by endoplasmic reticulum stress. *Oncogene* 2011;30:1147–58.
- 47 Crouse J, Kalinke U, Oxenius A. Regulation of antiviral T cell responses by type I interferons. *Nat Rev Immunol* 2015;15:231–42.
- 48 Jhunjhunwala S, Hammer C, Delamarre L. Antigen presentation in cancer: insights into tumour immunogenicity and immune evasion. *Nat Rev Cancer* 2021;21:298–312.
- 49 Cheng Q, Chang JT, Geradts J, *et al.* Amplification and high-level expression of heat shock protein 90 marks aggressive phenotypes of human Epidermal growth factor receptor 2 negative breast cancer. *Breast Cancer Res* 2012;14:R62.
- 50 Trepel J, Mollapour M, Giaccone G, *et al.* Targeting the dynamic HSP90 complex in cancer. *Nat Rev Cancer* 2010;10:537–49.
- 51 Li ZN, Luo Y. HSP90 inhibitors and cancer: prospects for use in targeted therapies (review). *Oncol Rep* 2023;49:6.
- 52 Mbofung RM, McKenzie JA, Malu S, *et al.* HSP90 inhibition enhances cancer immunotherapy by upregulating interferon response genes. *Nat Commun* 2017;8:451.
- 53 Schirrmacher V. From chemotherapy to biological therapy: a review of novel concepts to reduce the side effects of systemic cancer treatment (review). *Int J Oncol* 2019;54:407–19.
- 54 Kroemer G, Galluzzi L, Kepp O, *et al.* Immunogenic cell death in cancer therapy. *Annu Rev Immunol* 2013;31:51–72.
- 55 Zappasodi R, Merghoub T, Wolchok JD. Emerging concepts for immune checkpoint blockade-based combination therapies. *Cancer Cell* 2018;33:581–98.